Journal of Inorganic and Organometallic Polymers and Materials, Vol. 17, No. 1, March 2007 (© 2007)
DOI: 10.1007/s10904-006-9075-2

Metallo-Supramolecular Polymerization: A Route to Easy-to-Process Organic/Inorganic Hybrid Materials

Mark Burnworth,[1] Daniel Knapton,[1] Stuart J. Rowan,[1,2,3] and Christoph Weder[1,2,3]

Submitted: September 7, 2006; Accepted: October 17, 2006

The self-assembly polymerization of ditopic macromolecules via metal–ligand binding is a facile route for the preparation of metallo-supramolecular polymers (MSPs). We herein review our recent work focused on the synthesis and investigation of metallo-supramolecular polymers based on 2,6-bis(1′-methylbenzimidazolyl)pyridine endcapped poly(*p*-phenylene ethynylene) and poly(*p*-xylene) macromonomers. These materials are readily solution-processable and display appreciable mechanical properties as well as other attractive properties such as specific opto/electrical functions or high thermal stability. Our work illustrates that metallo-supramolecular polymerization offers an attractive approach to assemble high-molecular-weight macromolecules from well-defined, easy to process precursors. Variation of the ditopic ligands and metal ions allows one to easily tailor the desired properties.

KEY WORDS: conjugated polymer; metallopolymer; organic/inorganic hybrid material; organometallic; polymer; poly(*p*-phenylene ethynylene); poly(*p*-xylylene); PPE; PPX; processing; supramolecular polymerization; transition metal

1. INTRODUCTION

Triggered by the pioneering work of Ian Manners and others, significant research efforts have recently been focused on the synthesis and investigation of metallopolymers [1, 2]. In fact, due to their potential usefulness in a plethora of applications that range from catalysis to light-emitting devices to sensory materials, metallopolymers have become a most prominent research theme at the interface of metal-organic chemistry and polymer science. Main-chain conjugated metallopolymers are an interesting class of materials with desirable electronic and mechanical properties [3]. One important subset of metallopolymers is the class of metallo-supramolecular polymers (MSPs) [4], which encompasses metal-containing polymers in which the metal–ligand interaction is dynamic in nature and thus acts as the supramolecular motif. Utilizing a variety of non-covalent interactions, several recent studies have demonstrated that virtually any type of building block can be assembled with supramolecular motifs, yielding polymer materials that span a broad range of structures and properties [5]. Metal–ligand interactions represent a particularly useful and well-studied means of preparing supramolecular polymers (Scheme 1) [6–10]. A wide variety of metal–ligand binding motifs is available that offers a broad range of binding characteristics (e.g., thermodynamic and kinetic stabilities) [11], which in turn can be utilized to tune the nature of the resulting supramolecular materials [12]. Interestingly, however, reports of metallo-supramolecular conjugated polymers with appreciable mechanical properties appear to be rare. With the objective to develop new organic/inorganic hybrid materials, which combine good mechanical properties and other attractive properties (e.g., high

[1] Department of Macromolecular Science and Engineering, Case Western Reserve University, 2100 Adelbert Road, Kent Hale Smith Building, Cleveland, OH 44106-7202, USA.
[2] Department of Chemistry, Case Western Reserve University, 2100 Adelbert Road, Cleveland, OH 44106, USA.
[3] To whom correspondence should be addressed. E-mail: stuart.rowan@case.edu, christoph.weder@csae.edu

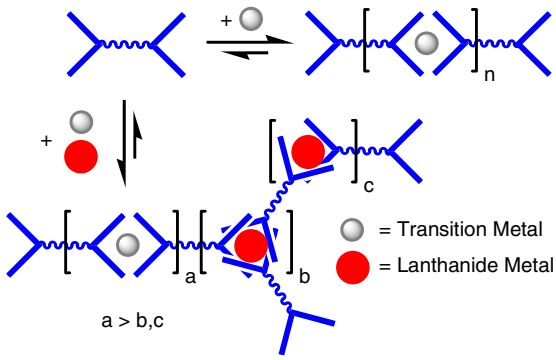

Scheme 1. Schematic representation of the metallo-supramolecular polymerization of ditopic ligands with transition and lanthanide metal ions.

stability at elevated temperatures, specific opto/electronic functions) with ease of processing, we embarked on the exploration of various new classes of metallo-supramolecular polymers. The general design approach attempts to merge the structure of known polymer systems, for example thermally stable hydrocarbon polymers or semiconducting polymers, with the advantages of a dynamic (reversible) polymerization process [13], to allow access to materials that are otherwise difficult to process [14]. We herein summarize our recent activities focused on the synthesis and investigation of metallo-supramolecular conjugated polymers and high-temperature stable poly(arylene alkylene)s prepared by this approach [15–18]. Our study made use of the following building blocks (Scheme 2): (i) ditopic macromonomers based on low-molecular-weight poly(2,5-dialkoxy-*p*-phenylene ethynylene) (PPE) (**1b**) or poly(2,5-dioctyloxy-*p*-xylylene) (PPX) (**2b**) segments; (ii) low-molecular model compounds mimicking either the basic *p*-phenylene ethynylene (**1a**) or *p*-xylylene unit (**2a**); (iii) the 2,6-bis(1′-methylbenzimidazolyl)pyridine (Mebip) ligand as the binding unit; and (iv) $Zn(ClO_4)_2$, $Fe(ClO_4)_2$, and/or $La(ClO_4)_3$, which cause

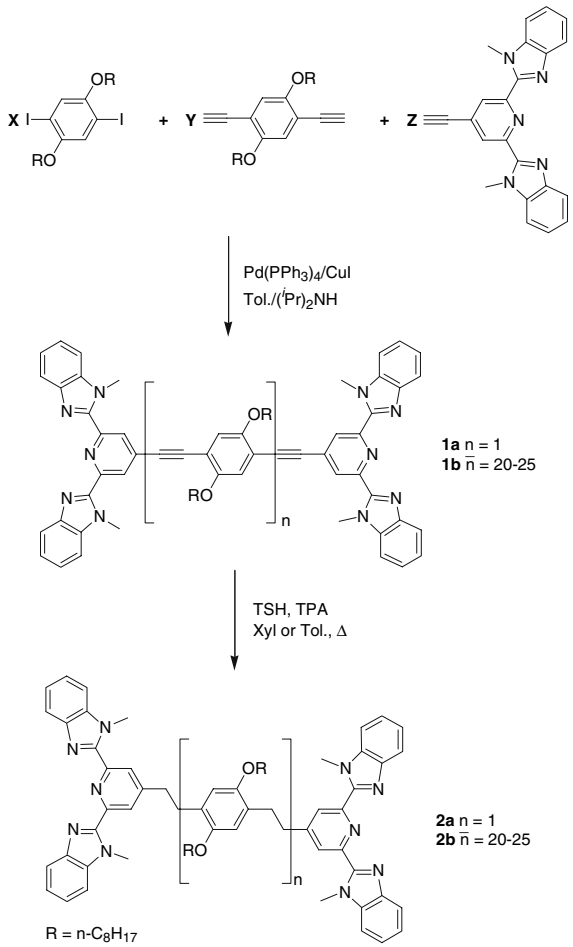

Scheme 2. Synthesis and molecular structures of the Mebip end-capped PPE and PPX (macro)monomers **1** and **2**.

linear chain extension (Zn^{2+} and Fe^{2+}) or branching/crosslinking (La^{3+}). The new metallopolymers prepared by these low-molecular-weight building blocks can be readily solution-processed and represent illustrative examples for metallo-supramolecular polymers with good mechanical properties.

2. SUPRAMOLECULAR POLY(*P*-PHENYLENE ETHYNYLENE)S

Since the discovery of electrical conductivity in π-conjugated polymers three decades ago [19], (semi)conducting polymers have become the focus of major research and development activities around the globe [20]. The excitement for this new generation of polymeric materials reflects their potential to combine the processability and outstanding properties of polymers with the exceptional, readily tailored electronic and optical properties of functional organic molecules. In particular their potential utilization as synthetic metals [21] and as organic semiconductors in light-emitting diodes [22], field-effect transistors [23], photovoltaic cells [24], sensors [25], and other devices have motivated the development of synthesis and processing methods of conjugated polymers with unique electronic properties. Unfortunately, high-molecular-weight conjugated polymers typically display high thermal transition temperatures, limited solubility, and high solution viscosity, and processing of these materials is therefore often intricate and time-consuming [26]. Furthermore, it is sometimes difficult to avoid structural defects in these macromolecules and/or to appropriately purify the materials, and hence, defective sequences disrupting the conjugation are not uncommon [27]. Low-molecular-weight conjugated polymers or oligomers are therefore frequently employed [28], but these materials lack of chain entanglements preventing the expression of "typical polymer properties" [29]. As a result, the mechanical properties of these (semi)conductors are inferior compared to conventional plastics. The framework of dynamic (reversible) polymerization is an attractive approach to solve this dilemma, since it allows one to assemble high-molecular weight macromolecules from well-defined, easy-to-process precursors. To explore this opportunity, we embarked on the metallo-supramolecular polymerization of conjugated macromonomers that were derived by functionalizing a low-molecular weight poly(2,5-dialkoxy-*p*-phenylene ethynylene) core – as a representative of an intensely investigated class of conjugated polymers [30] – with 2,6-bis(1′-methyl-benzimidazolyl)pyridine (Mebip) ligands on the two terminal positions (Scheme 2, **1b**) [16]. The Mebip moiety was chosen as it has been demonstrated to be a most versatile metal ion binding motif in supramolecular polymerizations [31] and also offers high thermal stability [32]. Reference materials using the ditopic model monomer **1a**, which mimics an isolated *p*-phenylene ethynylene unit, were also studied [15].

The model monomer **1a** and the Mebip end-capped PPE macromonomer **1b** are readily synthesized by the Sonogashira coupling of 2,5-dicotyloxy-1, 4-diiodobenzene, 1,4-diethynyl-2,5-bis(octyloxy) benzene with 2,6-bis(1′-methylbenzimidazolyl)-4-ethynyl-pyridine as an end capper (Scheme 2) [15, 16]. In view of the low solubility of high-molecular-weight PPEs with octyloxy side-chains [33], the number-average degree of polymerization, X_n, of **1b** was limited to 20–25 by slightly off-setting the molar ratio of the two bifunctional monomers and the use of appropriate amounts of the ligand end capper.

2.1. Optical Properties of Monomer 1a and Macromonomer 1b

Model monomer **1a** exhibits electronic properties that are significantly different from those of Mebip ligands, which are not further conjugated [15, 31, c]. The UV-vis absorption spectrum of **1a** in solution (Fig. 1a) shows a band associated with the Mebip moiety ($\lambda^{abs}{}_{max}$ = 321 nm) and additionally displays transitions at 352 and 390 nm, which appear to originate from the chromophore constituted by the Mebip ligands and the 1,4-diethynylphenylene (DPE) bridge [7, 34, 35]. Monomer **1a** displays a much stronger fluorescence than electronically isolated Mebip ligands. The emission associated with the isolated Mebip moieties (around 368 nm) is virtually absent; instead, an emission band at 448 nm is observed, which (through excitation scans) can be linked to the electronic transition (presumably π–π*) that is also responsible for the lowest-energy absorption (Fig. 1a).

The solution absorption spectrum of macromonomer **1b** exhibits a main band centered at 448 nm and a weaker band around 319 nm (Fig. 1b). These transitions are associated with the π–π* and n–π* transition of the polymer backbone, respectively [33]. Optical excitation of **1b** causes intense photoluminescence. The emission spectrum displays two well-resolved bands near 484 and 510 nm and exhibits

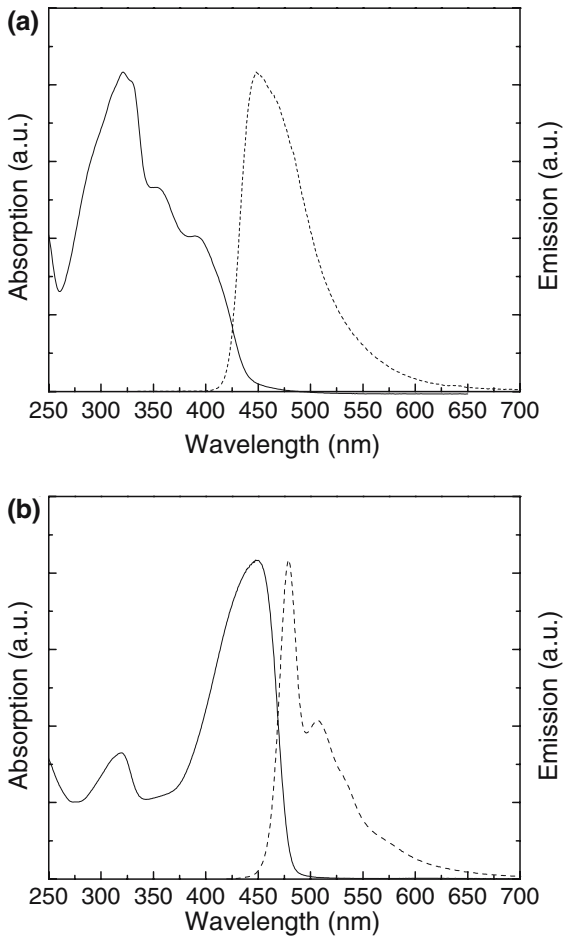

Fig. 1. UV-vis absorption (solid lines) and PL emission (dashed lines) spectra of (a) model compound **1a** and (b) macromonomer **1b** measured in $CHCl_3$.

features that are consistent with π–π* fluorescence. A comparison between the optical data of **1b** and a similar poly(2,5-dioctyloxy-*p*-phenylene ethynylene) without the Mebip end groups [33] reveals that these materials display virtually identical optical characteristics and that the Mebip end groups do not significantly alter the electronic properties of the PPE backbone.

2.2. Supramolecular Polymerization of Monomer 1a and Macromonomer 1b

The formation of metallo-supramolecular polymers of the type $[\mathbf{1a} \cdot MX_2]_n$ [15] and $[\mathbf{1b} \cdot MX_2]_n$ [16] is readily achieved by the addition of an acetonitrile solution of the metal ion salt to a chloroform solution of (macro)monomer **1a** or **1b**. A variety of metal ions display appropriate interactions (i.e., large equilibrium constant and relatively rapid complexation kinetics) that allow for supramolecular polymerization utilizing the terdentate Mebip motif [31]. In our study, we employed Zn^{2+} or Fe^{2+}, with the intent to probe the influence of the different electronic characteristics of these metals on the resulting metallopolymers. Zn^{2+} features a fully occupied d-orbital ($3d^{10}$) and is a prototype for metals that show hardly any tendency for metal-to-ligand charge transfer (MLCT) with imine-type ligands [36]. By contrast, Fe^{2+} is well known to form pronounced MLCT complexes and to act as a strong fluorescence quencher [37].

With the goal of attaining insight into the mechanism of the metal-ion-mediated self-assembly processes of these ditopic ligands, we titrated $Zn(ClO_4)_2$ into solutions of **1a** and examined the resulting products by means of UV-vis absorption and PL spectroscopy (Fig. 2) [15]. At a concentration of 10 μM the titration of **1a** with up to 1 eq. of Zn^{2+} rendered the originally colorless solution orange. Concomitantly, the lowest-energy absorption of the monomer is red-shifted to ca. 421 nm (Fig. 2a), consistent with either an intra-ligand charge transfer (CT) occurring from the electron-rich arylethynylene core to the electron-poor metal-bound Mebip moieties [38, 39], or a narrowing of the π–π* transition upon metal binding on account of stabilization of the π* molecular orbital [40]. Irrespective of the mechanism, the electron density on the ligand is a key factor for the large bathochromic shift [18]. The titration data further reveal a shift of the two other absorption bands to 404 and 339 nm (Fig. 2a); the appearance of three isosbestic points suggests equilibria between a finite number of spectroscopically distinct species. Upon addition of Zn^{2+}, the intensities of the new peaks increase in linear fashion, until a metal-to-monomer ratio of 1:1 is reached (Fig. 2a). Beyond this point, the subsequent addition of Zn^{2+} causes new spectral changes (Fig. 2b). The lowest-energy absorption is further red-shifted to 441 nm, while the 404 peak shifts to ca. 390 nm and the 339 nm peak appears to split into two bands at ca. 345 and 317 nm. The spectral changes level off at a metal-to-monomer ratio of 2:1. Isosbestic points are again observed, but they occur at different wavelengths than seen for the titration at metal-to-monomer ratios of below 1:1, indicating equilibration between a different set of spectroscopically distinct species. Thus, these data are consistent with the fact that at a 1:1 Zn^{2+}:**1a** ratio a metallo-supramolecular complex has formed, in which each Zn^{2+} is complexed with two monomers, and the resulting $[\mathbf{1a} \cdot Zn(ClO_4)_2]$

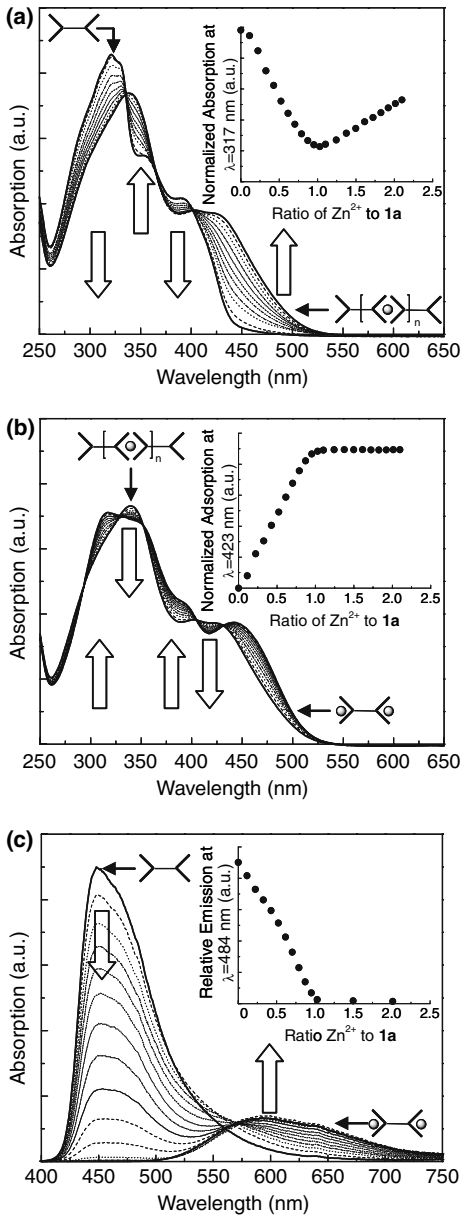

Fig. 2. UV-vis absorption spectra acquired upon titration of **1a** (10 μM) with $Zn(ClO_4)_2$. Shown are spectra at selected Zn^{2+}:**1a** ratios ranging from 0:1 to 1:1 (a) and from 1:1 to 2:1 (b). The insets show the normalized absorption at 317 nm (a) and 423 nm (b) as function of Zn^{2+}:**1a** ratio. (c) PL emission spectra (at selected Zn^{2+}:**1a** ratios of 0:1–2:1) acquired upon titration of **1a** (10 μM) in CH_3CN:$CHCl_3$ (1:9 v/v) with $Zn(ClO_4)_2$. The inset shows the normalized emission intensity at 484 nm as function of Zn^{2+}:**1a** ratio.

repeat unit is the origin of the observed dominating electronic transitions. At metal:**1a** ratios of above 1:1, depolymerization occurs, driven by the formation of the chain-terminating **1a**–Zn^{2+}-solvent complexes. Insets in Figs. 2a and 2b show the absorption changes at two selected wavelengths, highlighting the different nature of the predominant species involved in the self-assembly process at Zn^{2+}:**1a** ratios of below and above 1:1. It should be noted that the high extinction coefficient of **1a** dictated rather low concentrations (10 μM) for the above discussed optical experiments. As a result, these conditions clearly favor the formation of oligomeric species, as opposed to high-molecular weight macromolecules. In fact, as discussed above, the UV data nicely reflect a linear combination of absorption spectra associated with three distinctly different chromophores that we assign as free ligand, 1:1 Zn^{2+}:**1a** and 1:2 Zn^{2+}:**1a** complex. The relative contribution of these species was found to depend on the concentration of Zn^{2+} in the expected manner.

Metal-binding also exerts a pronounced influence on the emission characteristics of **1a**, as is evident from the PL spectra observed upon titration of $Zn(ClO_4)_2$ into a solution of **1a** (Fig. 2c). The emission maximum is strongly red-shifted from 448 nm to ca. 594 nm and experiences significant broadening. Similar to the absorption titration experiment for the same system, the emission spectra gradually change as the metal-to-**1a** ratio is increased. At a ratio of 1:1 the emission of the uncomplexed monomer has completely disappeared (Fig. 2c inset). Interestingly, in contrast to the absorption data, subsequent addition of Zn^{2+} results in no further spectral changes. This behavior is consistent with the fact that essentially irrespective of the relative amount of Zn^{2+}, emission occurs always from the same low-energy electronic states, presumably the **1a**–Zn^{2+}-solvent complexes referred to above.

Evidence for the formation of metallo-supramolecular polymers at higher concentrations comes from viscosity data (Fig. 3) for a series of solutions with different $Zn(ClO_4)_2$:**1a** ratios. The data (acquired at constant total solute concentration) show a steady increase of the reduced viscosity up to a Zn^{2+}:**1a** ratio of 1. Beyond this point a decrease in the reduced viscosity is observed, confirming the depolymerization of the supramolecular polymer. As expected, macromonomer **1b** also polymerizes readily if exposed to Zn^{2+} or Fe^{2+} and pronounced visual changes are observed [16]; the addition of an equimolar amount of Zn^{2+}, dissolved in CH_3CN, to a solution of **1b** in $CHCl_3$ (38.5 mg/mL) resulted in an instantaneous and significant increase of the solution's viscosity. To ensure processability of the resulting metallopolymer by attenuating its molecular weight, a slightly higher

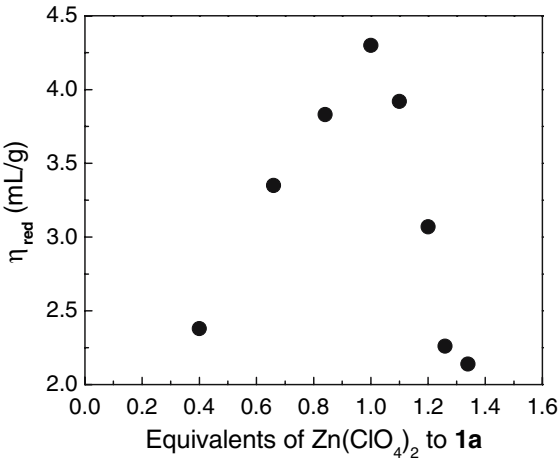

Fig. 3. Reduced viscosities of a series of dimethylacetamide solutions comprising $Zn(ClO_4)_2$ and **1a** at different molar ratios. The total concentration of solute was kept constant at 35 mg mL^{-1}.

than stoichiometric amount (1.04 equiv) of Zn^{2+} relative to the Mebip units present was employed. Evaporation of the solvent led to a red solid, which displayed appreciable mechanical properties. This metallopolymer could be re-dissolved in $CHCl_3$ and the resulting solutions were employed to produce (i) thin films for optical experiments by spin-coating (thickness <1 μm), (ii) free-standing films (thickness ca. 60 μm) for mechanical experiments by solution-casting, and (iii) monofilaments by simple solution spinning. These samples, shown in Fig. 4, visualize unequivocally that $[\mathbf{1b}\cdot Zn(ClO)_4]_n$ - very much in contrast to the neat macromonomer **1b** and a poly(2,5-dioctyloxy-*p*-phenylene ethynylene) of similar X_n but without the Mebip end groups [33] – offers considerable mechanical strength and flexibility. Metallopolymers based on **1b** and Fe^{2+} were prepared in a fashion similar to those of Zn^{2+}. This led to the instantaneous formation of a green mixture and a significant increase of the solution's viscosity. In this case, the solution was directly processed into thin films for optical experiments by spin-coating and freestanding films (thickness ca. 110 μm, Fig. 4c) for mechanical experiments by solution-casting.

The solid-state optical absorption spectrum of a $[\mathbf{1b}\cdot Zn(ClO_4)_2]_n$ film prepared by spin-casting from a $CHCl_3$ solution (not shown), exhibits essentially the same features as a thin film of the neat macromonomer **1b**, i.e., broad bands around 453 and 321 nm and a narrow aggregation band at 484 nm, suggesting that the band gap of the conjugated PPE sequences remains essentially unchanged upon binding of **1b** with Zn^{2+}. In order to compare the Zn^{2+}-mediated self-assembly process of **1b** with that of **1a**, $Zn(ClO_4)_2$ was titrated into a solution of **1b**, and the resulting products were analyzed by means of PL spectroscopy (Fig. 5). It should be noted that the precipitation of high-molecular-weight macromolecules at increased concentrations dictated that the PL titration experiment be performed at rather low concentrations

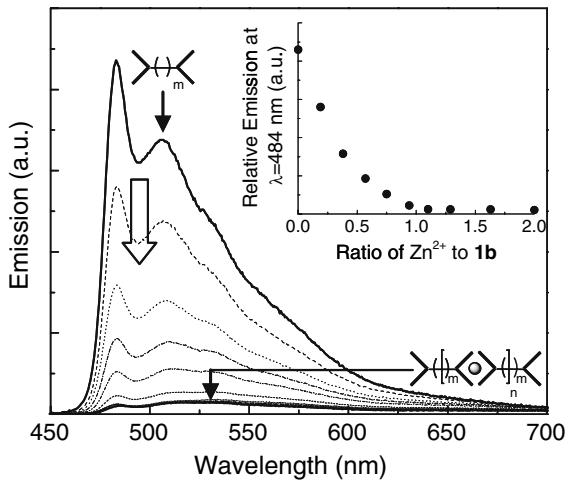

Fig. 5. PL emission spectra acquired upon titration of **1b** (0.022 mM) with $Zn(ClO_4)_2$ (excitation at 400 nm). Shown are spectra at selected Zn^{2+}:**1b** ratios of 0:1 to 2:1. The inset shows the normalized emission intensity at 484 nm as function of Zn^{2+}:**1b** ratio.

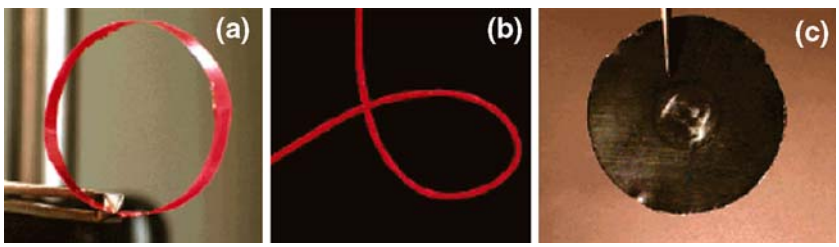

Fig. 4. (a) A film and (b) fiber of the metallo-supramolecular polymer $[\mathbf{1b}\cdot Zn(ClO_4)_2]_n$ and (c) a film of the metallo-supramolecular polymer $[\mathbf{1b}\cdot Fe(ClO_4)_2]_n$.

(22 μM). As such, these conditions clearly favor the formation of oligomeric species as opposed to high-molecular-weight aggregates. Figure 5 reveals that the emission associated with the PPE moieties is strongly quenched upon addition of Zn^{2+}. The inset of Fig. 5, which displays the relative emission intensity at $\lambda^{abs}{}_{max}$ (484 nm) as a function of Zn^{2+}, nicely shows that the effect depends on the concentration of Zn^{2+} in a nonlinear fashion and levels off at a Zn^{2+}:**1b** ratio of 1:1, at which point the emission observed for the neat **1b** is almost completely quenched. In the light of the above-discussed behavior of model monomer **1a**, these titration data are indicative of the formation of a metallosupramolecular complex of the form $[\mathbf{2}\cdot Zn(ClO_4)_2]_n$.

A comparison of the solid-state optical properties of $[\mathbf{1b}\cdot Fe(ClO_4)_2]_n$ and the neat macromonomer **1b** reveals the expected similarities and differences. The absorption spectrum (Fig. 6) shows that the transitions associated with the PPE backbone – broad bands around 445 and 320 nm and a narrow aggregation band at 476 nm – remain essentially unchanged. A characteristic [41] metal-to-ligand charge-transfer absorption band centered at 635 nm can be observed, which is absent in case of $[\mathbf{1b}\cdot Zn(ClO_4)_2]_n$. This MLCT band is indicative of the formation of the 2:1 Mebip:Fe^{2+} complex, which, of course, is the basis for the formation of the targeted supramolecular polymer [7]. It is well known that the latter complex is prone to dissipate excited-state energy through non-radiative processes; concomitantly $[\mathbf{1b}\cdot Fe(ClO_4)_2]_n$ does not fluoresce.

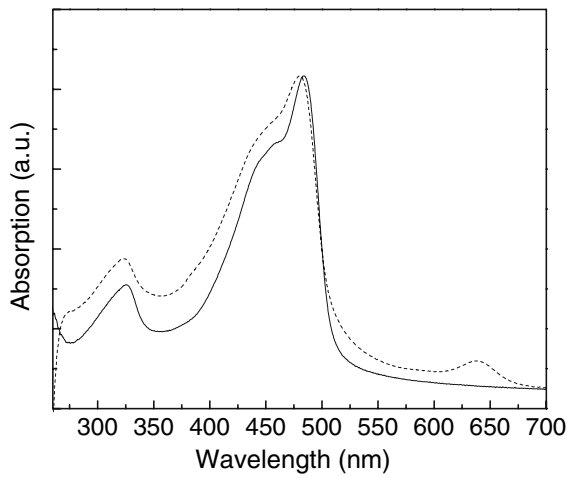

Fig. 6. UV-vis absorption spectra of metallopolymer $[\mathbf{1b}\cdot Fe(ClO_4)_2]_n$ measured on a spin-cast thin film (dashed) and macromonomer **1b** (solid).

2.3. Thermomechanical Properties of $[\mathbf{1b}\cdot Zn(ClO_4)_2]_n$ and $[\mathbf{1b}\cdot(Fe(ClO_4)_2]_n$

The thermal and mechanical properties of the supramolecular polymers $[\mathbf{1b}\cdot Zn(ClO_4)_2]_n$ and $[\mathbf{1b}\cdot(Fe(ClO_4)_2]_n$ and the parent macromonomer **1b** were investigated by means of thermogravimetric analysis (TGA) and dynamic mechanical thermoanalysis (DMTA) [16]. TGA traces of the neat macromonomer **1b** (Fig. 7a) acquired under N_2 reveal an onset of significant weight loss (2%) at 363 °C, corresponding to the thermal degradation of the polymer side chains. This experiment suggests outstanding thermal stability for the PPE building block, but it should be noted that thermal cross-linking of the ethynylene

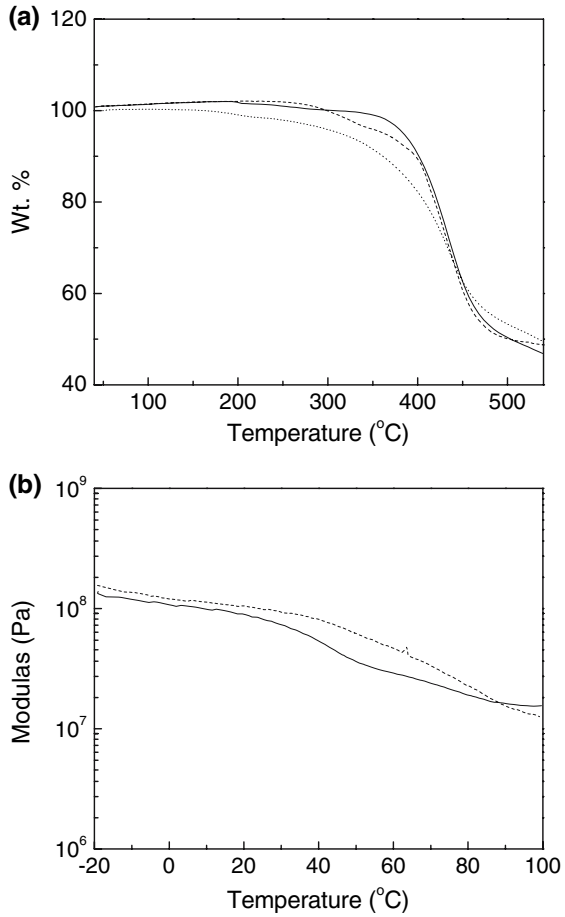

Fig. 7. (a) Thermogravimetric analysis (TGA) traces of **1b** (solid), $[\mathbf{1b}\cdot Zn(ClO_4)_2]_n$ (dashed), and $[\mathbf{1b}\cdot Fe(ClO_4)_2]_n$ (dotted). The experiments were conducted under N_2 at a heating rate of 20 °C/min. (b) Dynamic mechanical thermoanalysis (DMTA) traces of $[\mathbf{1b}\cdot Zn(ClO_4)_2]_n$ (dashed) and $[\mathbf{1b}\cdot Fe(ClO_4)_2]_n$ (solid). The experiments were conducted under N_2 at a heating rate of 3 °C/min and a frequency of 1 Hz.

units, which cannot be discerned by TGA, typically occurs at temperatures above 150 °C. The Zn^{2+} and Fe^{2+} metallopolymers (Fig. 7a) show a rather similar thermal behavior, but the 2% weight loss occurs at somewhat lower temperatures (313 and 250 °C, respectively), particularly in the case of Fe^{2+}. We ascribe this situation to the thermal degradation of the perchlorate counterions. We speculate that the significantly lower 2% weight loss temperature of the Fe^{2+} metallopolymer (compared to the Zn^{2+} system) may be due to a catalytic effect of the metal on the thermal decomposition of the perchlorate ions [42]. With the objective to maximize the thermal stability, we are considering investigating the influence of the counterion in more detail.

Gratifyingly, both $[\mathbf{1b} \cdot Zn(ClO_4)_2]_n$ and $[\mathbf{1b} \cdot (Fe(ClO_4)_2]_n$ films display sufficient mechanical strength to allow for characterization by DMTA (Fig. 7b). Experiments were conducted in a temperature range of −20 to 100 °C. The moduli of $[\mathbf{1b} \cdot Zn(ClO_4)_2]_n$ and $[\mathbf{1b} \cdot (Fe(ClO_4)_2]_n$ were determined to be ca. 160 and ca. 140 MPa at −20 °C and ca. 100 and ca. 83 MPa at 25 °C, respectively. A decrease of the modulus of both materials was observed over the experimental temperature range; $[\mathbf{1b} \cdot (Fe(ClO_4)_2]_n$ exhibits a distinguishable transition at ~40 °C, which, in view of the striking similarity to the DMTA trace of a high-molecular-weight poly(2,5-dialkoxy-*p*-phenylene ethynylene) (M_n ~83,000 g mol^{-1}) reported before [43], is tentatively assigned to a glass transition. The moduli of $[\mathbf{1b} \cdot Zn(ClO_4)_2]_n$ and $[\mathbf{1b} \cdot (Fe(ClO_4)_2]_n$ are similar to that of the latter polymer, and appear to be among the highest reported for any metallo-supramolecular conjugated polymer to date.

3. SUPRAMOLECULAR POLY(*P*-XYLYLENE)S

As another example, we recently investigated metallo-supramolecular poly(arylene alkylene)s, which were targeted because of their potential usefulness as high-temperature stable materials [17]. Poly(*p*-xylylene) (PPX) [44] is the most prominent representative of the poly(arylene alkylene) family. This polymer and its derivatives are well-known for an appealing combination of high thermal stability, excellent solvent resistance, high degree of crystallinity, low dielectric permittivity, and outstanding barrier properties [45, 46]. In addition, PPX exhibits excellent mechanical properties with a Young's modulus and a tensile strength of ca. 2.4 GPa and 47 MPa, respectively [45]. Thus, PPX is an attractive material for many applications, including packaging of electronic components, medical device fabrication, and artifact conservation [45]. Unfortunately, broad industrial exploitation of PPX has been stifled on account of its intractability. Its high melting temperature (424 °C, which overlaps with the onset of thermal degradation) and poor solubility make conventional processing protocols virtually impossible [47, 48]. As a result, the only practical approach for the synthesis and processing of PPX is by chemical vapor deposition polymerization [49]. It appears that this dilemma can, again, be solved by utilizing a supramolecular polymerization process. Building on the above-described work regarding the metal-ligand based self-assembly of Mebip-terminated PPEs and exploiting a reaction methodology developed in our laboratories for the reduction of PPEs to their corresponding PPX derivatives [50], we utilized supramolecular metallopolymerization for the synthesis of arylene alkylene metallopolymers [17]. The two PPX building blocks used are the ditopic model monomer **2a** and a low-molecular-weight Mebip-terminated macromonomer comprising a poly(2,5-dioctyloxy-*p*-xylylene) segment (**2b**), in combination with $Zn(ClO_4)_2$, $Fe(ClO_4)_2$ and/or $La(ClO_4)_3$ (Schemes 1 and 2).

The Mebip end-capped xylylene monomers **2a** and **2b** were prepared from the corresponding PPE precursors **1a** and **1b** (cf. Section 2) via diimide reduction chemistry utilizing *p*-toluenesulfonylhydrazide (TSH) and tripropylamine (TPA) (Scheme 2) [49, 51]. A Mebip end-capped PPE with an X_n of ca. 20 was employed to afford a PPX of slightly higher X_n (ca. 25) after purification.

3.1. Self-Assembly and Solution Properties of the Metallo-Supramolecular Polymers of 2a and 2b

The formation of metallo-supramolecular species $[\mathbf{2a} \cdot MX_n]_n$ and $[\mathbf{2b} \cdot MX_n]_n$ is readily achieved by the addition of one equivalent of an appropriate metal ion salt to a solution of the Mebip end-capped xylylenes **2a** and **2b**. Encouraged by the successful metallopolymerization of Mebip-end-capped PPEs with Zn^{2+} and Fe^{2+}, we opted to employ these metal ions in the present study. To probe the complexation characteristics of **2a** and **2b**, we first conducted a detailed optical titration study with Zn^{2+}, which offers both a large equilibrium constant and rapid complexation kinetics. To this end, $Zn(ClO_4)_2$ was titrated into solutions of **2a** and **2b**, and the resulting products were analyzed by means of UV-vis

spectroscopy (Fig. 8). It should be noted that precipitation, presumably of high-molecular-weight macromolecules, was observed if these experiments were carried out in too concentrated solutions; this dictated that the UV-vis titrations be performed at a concentration of 22–25 μM of the respective ditopic ligands. As such, these conditions again favor the formation of oligomeric species as opposed to high-molecular-weight aggregates. The addition of Zn^{2+} to xylylenes **2a** and **2b** rendered the originally colorless solutions pale yellow. In both cases a new lowest-energy absorption band was observed, centered at 354 nm in the case of **2a** and 360 nm in the case of **2b** (Figs. 8 a and 8b, respectively). Concomitantly, in model compound **2a** the intensity of the initial absorption band with λ_{max} at 318 nm associated with the π–π* transition related to the Mebip moiety was significantly reduced upon binding, as was the related absorption of macromonomer **2b** observed as a shoulder at ~330 nm. The spectra of both titration series exhibit a single isosbestic point at ~340 nm up to Zn^{2+}:**2a** and Zn^{2+}:**2b** ratios of approximately 1:1, suggesting equilibria between the bound and unbound monomers **2a** and **2b**. At Zn^{2+}:**2** ratios of greater than one, new isosbestic points are observed, which appear to correspond to the presence of chain-terminating monomer-Zn^{2+}-solvent complexes formed upon depolymerization of the supramolecular species in the presence of an excess of metal [15]. We further quantified the spectral changes observed in the above-discussed Zn^{2+} titrations as the normalized intensity of the emerging absorption bands; the data are plotted in the insets of Fig. 8. Gratifyingly, the changes are virtually identical for the well-defined monodisperse model compound **2a** and the macromonomer **2b**, leveling off at a Zn^{2+}:**2a** and Zn^{2+}**:2b** ratio of 1:1, which is consistent with the ditopic nature of the monomers and the successful self-assembly in dilute solution. Similar titration data (not shown) were obtained upon addition of $Fe(ClO_4)_2$ to **2b**. In this case, a characteristic [7, 16, 31] metal-to-ligand charge-transfer absorption band was observed at 570 nm.

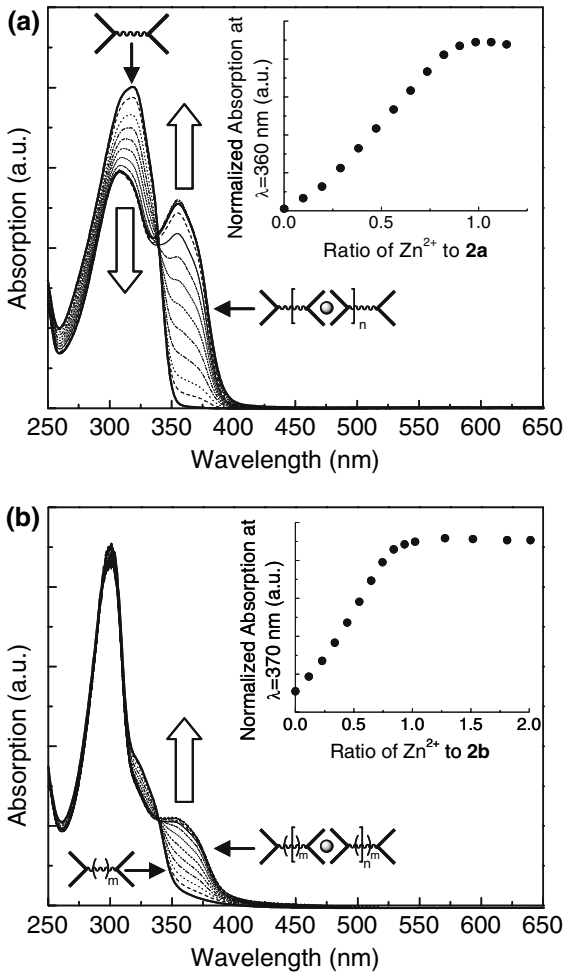

Fig. 8. UV-vis absorption spectra acquired upon titration of **2a** (0.025 mM) (a) and **2b** (0.022 mM) (b) with $Zn(ClO_4)_2$. Shown are spectra of Zn^{2+}:**2a** ratios between 0 and 1.14 and Zn^{2+}:**2b** ratios ranging from 0:1 to 1:2.01. The insets show the normalized absorption at 360 nm (a) and 370 nm (b) as a function of Zn^{2+}:**2a** and Zn^{2+}:**2b** ratio, respectively.

3.2. Preparation and Solid-State Optical Properties of Metallo-Supramolecular Polymers Based on 2b

Monomer **2b** is a pale yellow powder, which is soluble in chloroform and can readily be spin- or solution-cast into homogeneous thin films. However, this material does not display any self-supporting mechanical properties. The preparation and processing of metallo-supramolecular polymers based on **2b** and $Zn(ClO_4)_2$ or $Fe(ClO_4)_2$ ($[\mathbf{2b}\cdot M]_n$) followed the protocol developed for the metallopolymerization of Mebip-end-capped PPE **1b**, which resulted in materials with outstanding mechanical properties. The procedure involved co-dissolution of **2b** and an equimolar amount of either of the metal salts in a $CHCl_3/CH_3CN$ mixture, followed by solution casting. Interestingly, the addition of either $Zn(ClO_4)_2$ or $Fe(ClO_4)_2$ in CH_3CN to **2b** in $CHCl_3$ resulted in solutions of $[\mathbf{2b}\cdot Zn(ClO_4)_2]_n$ and $[\mathbf{2b}\cdot Fe(ClO_4)_2]_n$, which upon casting and drying yielded films that displayed poor mechanical properties (Fig. 9a). To probe whether an increase of the X_n of the macromo-

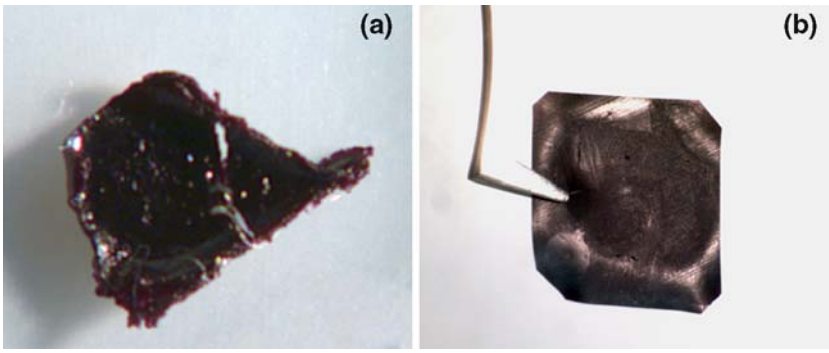

Fig. 9. Pictures of solution-cast films ($CHCl_3$) of the metallo-supramolecular polymers $[\mathbf{2b} \cdot Fe(ClO_4)_2]_n$ (a) and $[\mathbf{2b} \cdot Fe(ClO_4)_2/La(ClO_4)_3]_n$ (b).

nomer would change this situation, the experiment was repeated with a macromonomer **2b** of an X_n of ~32 instead of ~25, but the behavior of this ditopic ligand was virtually the same. Thus, the $[\mathbf{2b} \cdot M]_n$ samples display mechanical properties that are clearly inferior when compared with the corresponding $[\mathbf{1b} \cdot M]_n$ analogues. The structural purity of **2b** established by NMR, the successful self-assembly in dilute solution established by optical titration, and the fact that the binding strength of **2b** should be similar to that of **1b** and many related systems [31] suggests that the $[\mathbf{2b} \cdot M]_n$ supramolecular materials prepared here are indeed of polymeric nature. Thus, the observation of poor mechanical properties seems to reflect the lack or low concentration of chain entanglements and indicates weak intermolecular interactions between the individual supramolecular chains.

With the objective to improve the material's mechanical properties, we employed minor amounts of lanthanide perchlorate salts, which are well-known to bind three Mebip ligands [52], as a cross-linking/branching unit in our supramolecular polymerization of **2b** and $Fe(ClO_4)_2$ (Scheme 1). To generate the crosslinks/branch points in a metal ion:**2b** system that was processed as described above, 9 mol% $La(ClO_4)_3$ (with respect to **2b**) in CH_3CN was added to xylylene **2b** in $CHCl_3$ (71.4 mg/mL) with the assumption of a 3:1 Mebip:La^{3+} binding motif. The further addition of 91 mol% $Fe(ClO_4)_2$ in CH_3CN resulted in an instantaneous and dramatic visual increase of the solution's viscosity, illustrating the successful linear chain growth (via 2:1 Mebip:**2b** binding) of the preformed 3:1 Mebip:La^{3+} complexes. Solution casting and slow evaporation of the solvent led to purple films, which displayed appreciable mechanical properties (Fig. 9b) in stark contrast to neat **2b** and poly(2,5-dioctyloxy-*p*-xylylene) [50] of similar X_n but without Mebip end groups. The deep purple color of the material results from a MLCT, indicative of the formation of 2:1 Mebip:Fe^{2+} complexes, as the addition of $La(ClO_4)_3$ to **2b** resulted in the formation of only near colorless solutions [7, 16, 31]. As a consequence of non-radiative energy dissipation processes associated with the MLCT complex involving iron, $[\mathbf{2b} \cdot Fe(ClO_4)_2]_n$ and $[\mathbf{2b} \cdot Fe(ClO_4)_2/La(ClO_4)_3]_n$ also do not fluoresce.

3.3. Thermomechanical Properties of $[\mathbf{2b} \cdot Fe(ClO_4)_2/La(ClO_4)_3]_n$

The mechanical and thermal properties of $[\mathbf{2b} \cdot Fe(ClO_4)_2/La(ClO_4)_3]_n$ films were investigated in more detail by means of thermogravimetric analysis (TGA), dynamic mechanical thermoanalysis (DMTA), and modulated differential scanning calorimetry (MDSC), all under N_2. TGA traces (Fig. 10a) of neat **2b** reveal an onset of significant weight loss (2%) at 354 °C, which has previously been related to the degradation of alkyl side chains [53]. The supramolecular polymer $[\mathbf{2b} \cdot Fe(ClO_4)_2/La(ClO_4)_3]_n$ shows a rather similar overall thermal behavior (Fig. 10a). However, the initial 2% weight loss was observed at a substantially lower temperature (193 °C), which we again ascribe to the thermal degradation of the perchlorate counterions upon melting. The mechanical properties of $[\mathbf{2b} \cdot Fe(ClO_4)_2/La(ClO_4)_3]_n$ were elucidated by DMTA in a temperature range of −20 to 100 °C (Fig. 10b). The room-temperature modulus was determined to be 220 MPa, placing the self-assembled system above the linear PPE metallopolymer discussed in Section 2 and in the same regime as low-density polyethylene. The modulus decreased continuously as the temperature was increased, which may be on account of progressive decomplexation of the more weakly bound lantha-

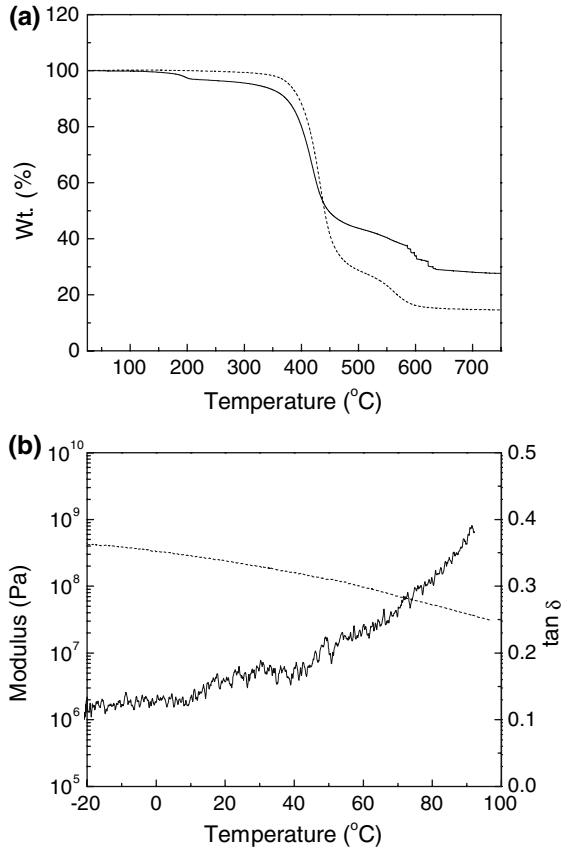

Fig. 10. (a) Thermogravimetric analysis (TGA) traces of [**2b**·Fe(ClO_4)$_2$/La(ClO_4)$_3$]$_n$ (solid) and xylylene **2b** (dashed). The experiments were conducted under N_2 at a heating rate of 10 °C/min. (b) Dynamic mechanical thermoanalysis (DMTA) trace (modulus: dashed, tan δ: solid) for [**2b**·Fe(ClO_4)$_2$/La(ClO_4)$_3$]$_n$. The experiment was conducted under N_2 at a heating rate of 3 °C/min and a frequency of 1 Hz.

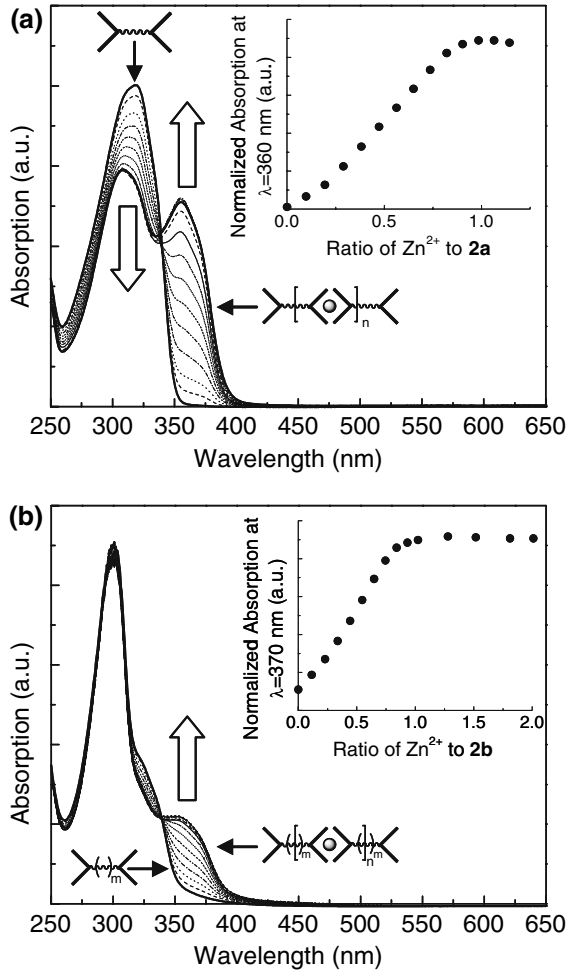

Fig. 11. Modulated differential scanning calorimetry (MDSC) heating scans of **2b** (a) and [**2b**·Fe(ClO_4)$_2$/La(ClO_4)$_3$]$_n$ (b) with nonreversible heat flow (solid), heat flow (dashed), and reversible heat flow (dotted). The experiments were conducted under N_2 at a heating rate of 2 °C/min.

nide-Mebip cross-links. To determine the melting temperature, T_m, of both **2b** and [**2b**·Fe(ClO_4)$_2$/La(ClO_4)$_3$]$_n$, MDSC experiments were performed (Fig. 11). The MDSC trace of neat **2b** clearly shows a reversible endotherm with maximum at 166 °C corresponding to the T_m, which is virtually identical to that reported for a poly(2,5-dioctyloxy-*p*-xylylene) of similar X_n but without Mebip end groups (170 °C) [50]. The MDSC trace of [**2b**·Fe(ClO_4)$_2$/La(ClO_4)$_3$]$_n$ shows a largely irreversible exotherm at 176 °C that we associate, by comparison with TGA data, to the degradation of the perchlorate counterions. The reversible portion of the scan shows a weak endotherm at 166 °C, which corresponds to melting at a temperature which is nearly identical to that of **2b.** Thus, the MDSC data suggest that the melt transition of the new metallo-supramolecular PPX is largely governed by the hydrocarbon building block and can be tailored to meet specific thermal demands by judicious design of the latter.

4. CONCLUSIONS

With the objective to develop new organic/inorganic hybrid materials, which combine good mechanical properties and other attractive characteristics (e.g., high stability at elevated temperatures, specific opto/electronic functions) with ease of processing, we embarked on the exploration of two new classes of metallo-supramolecular polymers. We have demonstrated that the supramolecular metallopolymerization of PPE- and PPX-type Mebip end-capped

macromolecules can be employed to create metallopolymers which are readily solution-processed and display good mechanical properties. The comparison of mechanical data acquired for the two series nicely illustrates how strongly the nature and interactions among the building blocks and the self-assembly characteristics of the metal ion affect the materials properties. Thus, metallosupramolecular polymerization not only offers an attractive approach to assemble high-molecular-weight macromolecules from well-defined, easy to process precursors, but the broad range of metal ions available allows one to easily tailor the desired properties. It appears that the use of such dynamic polymerizations offers a broadly useful means to attain thermally robust inorganic/organic hybrid materials without altering the properties associated with the macromolecular core and should be easily extendable to other thermally stable cores.

ACKNOWLEDGMENTS

This material is based upon work supported by the U.S. Army Research Office (DAAD19-03-1-0208). We acknowledge fruitful interactions with Drs. J. Benjamin Beck, Akshay Kokil, and Parameswar Iyer.

REFERENCES

1. (a) I. Manners, *Angew. Chem. Int. Ed. Engl.* **35**, 1602 (1996). (b) P. Nguyen, P. Gómex-Elipe, and I. Manners, *Chem. Rev.* **99**, 1515 (1999). (c) A. S. Abd-El-Aziz, C. E. Carraher, Jr., C. U. Pittman, Jr., M. Zeldin, in *Macromolecules Containing Metal and Metal-Like Elements*, (Wiley-Interscience, Hoboken, New Jersey, 2006), Vol. 1–7.
2. (a) D. A. Foucher, B.-Z. Tang, and I. Manners, *J. Am. Chem. Soc.* **114**, 6246 (1992). (b) Y. Ni, R. Rulkens, and I. Manners, *J. Am. Chem. Soc.* **118**, 4102 (1996). (c) J. A. Massey, K. Temple, L. Cao, Y. Rharbi, J. Raez, M. A. Winnik, and I. Manners, *J. Am. Chem. Soc.* **122**, 11577 (2000). (d) K. Kulbada and I. Manners, *Macromol. Rapid Commun.* **22**, 711 (2001).
3. (a) C. U. Pittman, *J. Inorg. Organomet. Polym. Mater.* **15**, 33 (2005). (b) C. Moorlag, B. B. Sih, T. L. Stott, and M. O. Wolf, *J. Mater. Chem.* **15**, 2433 (2005). (c) U. H. F. Bunz, *J. Organomet. Chem.* **683**, 269 (2003). (d) J. Roncalli, *J. Mater. Chem.* **9**, 1875 (1999). (e) P. G. Pickup, *J. Mater. Chem.* **9**, 1641 (1999). (f) A. J. Boydston and C. W. Bielawski, *Dalton Trans.* 4073 (2006).
4. U. S. Schubert, G. R. Newkome, and I. Manners *Metal-Containing and Metallosupramolecular Polymers and Materials* (ACS, Washington, D.C, 2006).
5. (a) L. Brunsveld, B. J. B. Folmer, E. W. Meijer, and R. P. Sijbesma, *Chem. Rev.* **101**, 4071 (2001). (b) A. Ciferri, *Macromol. Rapid Commun.* **23**, 511 (2002). (c) H. Hofmeier and U. S. Schubert, *Chem. Commun.* 2423 (2005). (d) H. Hofmeier, R. Hoogenboom, M. E. L. Wouters, and U. S. Schubert, *J. Am. Chem. Soc.* **127**, 2913 (2005). (e) M. A. R. Meier, D. Wouters, C. Ott, P. Guillet, C.-A. Fustin, J.-F. Gohy, and U. S. Schubert, *Macromolecules* **39**, 1569 (2006). (e) W. W. Gerhardt, A. J. Zucchero, J. N. Wilson, C. R. South, U. H. F. Bunz, and M. Weck, *Chem. Commun.* 2141 (2006).
6. (a) S. Kelch and M. Rehahn, *Macromolecules* **32**, 5818 (1999). (b) M. Rehahn, *Acta Polym.* **49**, 201 (1998). (c) B. Lahn and M. Rehahn, *Macromol. Symp.* **163**, 157 (2001). (d) R. Knapp, A. Schott, and M. Rehahn, *Macromolecules* **29**, 478 (1996). (e) U. Velten and M. Rehahn, *Chem. Commun.* 2639 (1996). (f) S. Schmatloch, A. M. J. van den Berg, H. Hofmeier, and U. S. Schubert, *Des. Monomers Polym.* **7**, 191 (2004). (g) H. Hofmeier, S. Schmatloch, D. Wouters, and U. S. Schubert, *Macromol. Chem. Phys.* **204**, 2197 (2003). (h) S. Schmatloch, A. M. J. van den Berg, A. S. Alexeev, H. Hofmeier, and U. S. Schubert, *Macromolecules* **36**, 9943 (2003). (i) J. M. Pollino, K. P. Nair, L. P. Stubbs, J. Adams, and M. Weck, *Tetrahedron* **60**, 7205 (2004). (j) W. Gerhardt, M. Èrne, and M. Weck, *Chem. Eur. J.* **10**, 6212 (2004).
7. A. El-ghayoury, A. P. H. J. Schenning, and E. W. Meijer, *J. Polym. Sci. A: Polym. Chem.* **40**, 4020 (2002).
8. (a) E. Figgemeier, L. Merz, B. A. Hermann, Y. C. Zimmermann, C. E. Housecroft, H.-J. Güntherodt, and E. C. Constable, *J. Phys. Chem. B* **107**, 1157 (2003). (b) E. C. Constable, C. E. Housecroft, M. Neuburger, A. G. Schneider, B. Springler, and M. Zehnder, *Inorg. Chim. Acta* **300--302**, 49 (2000). (c) E. C. Constable, C. E. Housecroft, J. N. Lambert, and D. A. Malarek, *Chem. Commun.* 3739 (2005). (d) J. Hjelm, R. W. Hel, A. Hagfeldt, E. C. Constable, C. E. Houscroft, and R. J. Forster, *Inorg. Chem.* **44**, 1073 (2005). (e) J. Hjelm, R. W. Handel, A. Hagfeldt, E. C. Constable, C. E. Housecroft, and R. J. Forster, *Electrochem. Commun.* **6**, 193 (2004). (f) J. Hjelm, E. C. Constable, E. Figgemeier, A. Hagfeldt, R. Handel, C. E. Housecroft, E. Mukhtar, and E. Schofield, *Chem. Commun.* 284 (2002). (g) S. Encinas, L. Flamigni, F. Barigelletti, E. C. Constable, C. E. Housecroft, E. Schofield, E. Figgemeier, D. Fenske, M. Neuburger, and J. G. Vos, M. Zehnder, *Chem. Eur. J.* **8**, 137 (2002).
9. (a) M. Schütte, D. G. Kurth, M. R. Linford, H. Cölfen, and H. Möhwald, *Angew. Chem., Int. Ed.* **37**, 2891 (1998). (b) D. G. Kurth, P. Lehmann, and M. Schütte, *Proc. Natl. Acad. Sci. U.S.A.* **97**, 5704 (2000). (c) P. Lehmann, D. G. Kurth, G. Brezesinski, and C. Symietz, *Chem. Eur. J.* **7**, 1646 (2001). (d) D. G. Kurth, A. F. Meister, A. F. Thünemann, and G. Förster, *Langmuir* **19**, 4055 (2003). (e) D. G. Kurth, N. Severin, and J. P. Rabe, *Angew. Chem., Int. Ed.* **41**, 3681 (2002).
10. R. Dobrawa, M. Lysetska, P. Ballester, M. Grüne, and F. Würthner, *Macromolecules* **38**, 1315 (2005).
11. (a) P. Nguyen, P. Gómes-Elipe, and I. Manners, *Chem. Rev.* **99**, 1515 (1999). (b) P. G. Pickup, *J. Mater. Chem.* **9**, 1641 (1999). (c) M. O. Wolf, *Adv. Mater.* **13**, 545 (2001). (c) U. S. Schubert and C. Eschbaumer, *Angew. Chem., Int. Ed.* **41**, 2892 (2002). (d) I. Manners, *Synthetic Metal-Containing Polymers* (Wiley-VCH, Weinheim, 2004). (e) E. Holder, B. M. W. Langeveld, and U. S. Schubert, *Adv. Mater.* **17**, 1109 (2005). (f) B. J. Holliday and T. M. Swager, *Chem. Commun.* 23 (2005).
12. (a) S. Schmatloch, M. F. González, and U. S. Schubert, *Macromol. Rapid Commun.* **23**, 957 (2002). (b) W. C. Yount, H. Juwarker, and S. L. Craig, *J. Am. Chem. Soc.* **125**, 15302 (2003). (c) T. Vermonden, J. van der Gucht, P. de Waard, A. T. M. Marcelis, N. A. M. Besseling, E. J. R. Sudhölter, G. J. Fleer, and M. A. C. Stuart, *Macromolecules* **36**, 7035 (2003). (d) B. Lahn and M. Rehahn, *e-Polym.* **1**, 1 (2002). (e) D. M. Loveless, S. L. Jeon, and S. L. Craig, *Macromolecules* **38**, 10171 (2005). (f) W. C. Yount, D. M. Loveless, and S. L. Craig, *J. Am. Chem. Soc.* **127**, 14488 (2005). (g) M. Schmittel, V. Kalsani, R. S. K. Kishore, H. Cölfen, and J. W. Bats, *J. Am. Chem. Soc.* **127**, 11544 (2005).
13. (a) S. J. Rowan, S. J. Cantrill, G. R. L. Cousins, J. K. M. Sanders, and J. F. Stoddart, *Angew. Chem., Int. Ed*, **41**, 898

(2002). (b) L. Brunsveld, B. J. B. Folmer, E. W. Meijer, and R. P. Sijbesma, *Chem. Rev.* **101**, 4071 (2001). (c) A. Ciferri, *Macromol. Rapid Commun.* **23**, 511 (2002).
14. A. Kokil, I. Shiyanovskaya, K. D. Singer, and C. Weder, *J. Am. Chem. Soc.* **124**, 9978 (2002).
15. P. K. Iyer, J. B. Beck, C. Weder, and S. J. Rowan, *Chem. Commun.* 319 (2005).
16. D. Knapton, S. J. Rowan, and C. Weder, *Macromolecules* **39**, 651 (2006).
17. D. Knapton, S. J. Rowan, and C. Weder, *Macromolecules* **39**, 4069 (2006).
18. D. Knapton, M. Burnworth, S. J. Rowan, and C. Weder, *Angew. Chem.* **45**, 5825 (2006).
19. H. Shirakawa, E. J. Louis, A. G. MacDiarmid, C. K. Chiang, and A. J. Heeger, *J. Chem. Soc., Chem. Commun.* 578 (1977).
20. (a) A. J. Heeger, *Rev. Mod. Phys.* **73**, 681 (2001). (b) A. G. MacDiarmid, *Rev. Mod. Phys.* **73**, 701 (2001). (c) H. Shirakawa, *Rev. Mod. Phys.* **73**, 713 (2001).
21. (a) H. S. Nalva, ed., in *Handbook of Organic Conductive Molecules and Polymers*, (Wiley, New York, 1996). (b) T. A. Skotheim, R. L. Elsenbaumer, and J. R. Reynolds, eds., in *Handbook of Conducting Polymers*, 2nd ed. (Dekker, New York, 1998).
22. (a) A. Kraft, A. C. Grimsdale, and A. B. Holmes, *Angew. Chem. Int. Ed.* **37**, 403 (1998). (b) U. Mitschke and P. Bäuerle, *J. Mater. Chem.* **10**, 1471 (2000). (c) A. Greiner and C. Weder, in *Encyclopedia of Polymer Science and Technology*, J. I. Kroschwitz, ed. (Wiley-Interscience, New York, 2001), Vol. 3, p. 87.
23. G. Horowitz, *Adv. Mater.* **10**, 365 (1998).
24. C. J. Brabec, N. S. Sariciftci, and J. C. Hummelen, *Adv. Funct. Mater.* **11**, 15 (2001).
25. D. T. McQuade, A. E. Pullen, and T. M. Swager, *Chem. Rev.* **100**, 2537 (2000).
26. (a) P. Smith and C. Weder, in *Encyclopedia of Materials: Science and Technology*, K. H. Buschow, R. W. Cahn, M. C. Flemings, B. Ilschner, E. J. Kramer, and S. Mahajan, eds. (Elsevier Science, Amsterdam, 2001), p. 1497.
27. (a) H. Becker, H. Spreitzer, K. Ibrom, and W. Kreuder, *Macromolecules* **32**, 4925 (1999). (b) U. H. F. Bunz, *Chem. Rev.* **100**, 1605 (2000). (c) E. J. W. List, R. Günther, P. Scanducci de Freitas, and U. Scherf, *Adv. Mater.* **14**, 374 (2002). (d) M. Gaal, E. J. W. List, and U. Scherf, *Macromolecules* **36**, 4236 (2003).
28. K. Müllen, and G. Wegner eds., *Electronic Materials: The Oligomer Approach* (Wiley-VCH, Weinheim, 1998).
29. A. T. Ten Cate and R. P. Sijbesma, *Macromol. Rapid Commun.* **23**, 1094 (2002).
30. C. Weder, ed., in *Poly(arylene ethynylene)s–From Synthesis to Applications*; *Adv. Polym. Sci.* (Springer, Heidelberg, 2005), Vol. 177.
31. (a) J. B. Beck and S. J. Rowan, *J. Am. Chem. Soc.* **125**, 13922 (2003). (b) Q. Y. Zhao, J. B. Beck, S. J. Rowan, and A. M. Jamieson, *Macromolecules* **37**, 3529 (2004). (c) S. J. Rowan and J. B. Beck, *Faraday Discuss.* **128**, 43 (2005). (d) J. B. Beck, J. M. Ineman, and S. J. Rowan, *Macromolecules* **38**, 5060 (2005). (e) W. Weng, J. B. Beck, A. M. Jamieson, and S. J. Rowan, *J. Am. Chem. Soc.* **128**, 11663 (2006).
32. (a) S. Petoud, J.-C. G. Bünzli, K. J. Schenk, and C. Piguet, *Inorg. Chem.* **36**, 1345 (1997). (b) H. Nozary, C. Piguet, P. Tissot, G. Bernardinelli, J.-C. G. Buenzli, R. Deschenaux, and D. Guillon, *J. Am. Chem. Soc.* **120**, 12274 (1998). (c) H. Nozary, C. Piguet, J.-P. Rivera, P. Tissot, G. Bernardinelli, N. Vulliermet, J. Weber, and J.-C. G. Buenzli, *Inorg. Chem.* **39**, 5286 (2000). (d) H. Nozary, C. Piguet, J.-P. Rivera, P. Tissot, P.-Y. Morgantini, J. Weber, G. Bernardinelli, J.-C. G. Buenzli, R. Deschenaux, B. Donnio, and D. Guillon, *Chem. Mater.* **14**, 1075 (2002). (e) E. Terazzi, S. Torelli, G. Bernardinelli, J.-P. Rivera, J.-M. Benech, C. Bourgogne, B. Donnio, D. Guillon, D. Imbert, J.-C. G. Buenzli, A. Pinto, D. Jeannerat, and C. Piguet, *J. Am. Chem. Soc.* **127**, 889 (2005).
33. C. Weder and M. S. Wrighton, *Macromolecules* **29**, 5157 (1996).
34. (a) A. Khatyr and R. Ziessel, *J. Org. Chem.* **65**, 3126 (2000); (b) C. Ringenbach, A. Di Nicola, and R. Ziessel, *J. Org. Chem.* **68**, 4708 (2003).
35. All electronic spectra were measured in CH_3CN–$CHCl_3$ (1:9 v/v).
36. F. M. Jaeger and J. A. Dijk, *Z. Anorg. Chem.* **227**, 273 (1938).
37. R. Dobrawa and F. Würthner, *Chem. Commun.* 1878 (2002).
38. X.-Y. Wang, A. Del Guerzo, and R. H. Schmehl, *Chem. Commun.* 2344 (2002).
39. J. N. Wilson and U. H. F. Bunz, *J. Am. Chem. Soc.* **127**, 4124 (2005).
40. C. Piguet, J.-C. G. Bünzli, G. Bernardinelli, C. G. Bochet, and P. Froidevaux, *J. Chem. Soc. Dalton Trans.* 83 (1995).
41. P. Krumholz, *Inorg. Chem.* **4**, 612 (1965).
42. S. A. Halawy and M. A. Mohamed, *Collect. Czech. Chem. Commun.* **59**, 2253 (1994).
43. D. Steiger, P. Smith, and C. Weder, *Macromol. Rapid Commun.* **18**, 643 (1997).
44. L. A. Errede and M. Szwarc, *Q. Rev. Chem. Soc.* **12**, 301 (1958).
45. W. F. Beach, in *Encyclopedia of Polymer Science and Technology*, 3rd ed., J. Kroschwitz, ed. (John Wiley & Sons, New York, 2004), Vol. 12, p. 587 ff.
46. A. Greiner, S. Mang, O. Schäfer, and P. Simon, *Acta Polym.* **48**, 1 (1997).
47. (a) L. A. Errede and N. Knoll, *J. Polym. Sci.* **60**, 21 (1962). (b) D. E. Kirkpatrick, B. Wunderlich, *Makromol. Chem.* **186**, 2595 (1985).
48. M. Szwarc, *Polym. Eng. Sci.* **16**, 473 (1976).
49. A. Greiner, *Trends Polym. Sci.* **5**, 12 (1997).
50. J. B. Beck, A. Kokil, D. Ray, S. J. Rowan, and C. Weder, *Macromolecules* **35**, 590 (2002).
51. (a) S. F. Hahn, *J. Polym. Sci. A: Polym. Chem.* **30**, 397 (1992). (b) M. A. Hillmyer, W. R. Laredo, and R. H. Grubbs, *Macromolecules* **28**, 6311 (1995). (c) K. B. Wagener, D. Valenti, and S. F. Hahn, *Macromolecules* **30**, 6688 (1997).
52. C. Piguet, A. F. Williams, G. Bernardinelli, and J.-C. G. Bünzli, *Inorg. Chem.* **32**, 4139 (1993).
53. W. Y. Huang, W. Gao, T. K. Kwei, and Y. Okamoto, *Macromolecules* **34**, 1570 (2001).